JOC The Journal of Organic Chemistry
Cite This: J. Org. Chem. 2019, 84, 8284−8288
Note
pubs.acs.org/joc

A Protonated Quinone Methide Stabilized by a Combination of Partial Aromatization and π-Interaction: Spectroscopic and Crystallographic Analysis

Muhammad Kazim, Maxime A. Siegler, and Thomas Lectka*

Department of Chemistry, Johns Hopkins University, 3400 North Charles Street, Baltimore, Maryland 21218, United States

Supporting Information

ABSTRACT: We have expanded the repertoire of cation−π interactions to include a carbocation−π system resulting from the protonation of a π-stacked *para*-quinone methide (p-QM). This unusual carbocation is stabilized by a combination of partial aromatization of the QM moiety and through-space interaction with the π-system of the adjacent aromatic ring. Single crystal X-ray analysis of the protonated form reveals a structure consisting of a hydrogen-bound complex involving two molecules of the precursor and one proton.

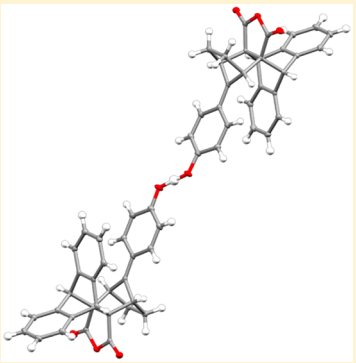

Noncovalent cation−π interactions are of prime importance in various areas of study such as chemistry, materials science, and biology.[1−6] Among the first recognized examples was reported in 1981 when Kebarle et al. showed that a naked K^+ ion in the gas phase binds preferentially to benzene over water.[7] The nascent field soon ramified greatly to include interactions of π-systems with other metal cations,[8] ammonium salts,[9,10] and sulfonium ions,[11] to name but a few examples. One region of the wide spectrum of potential interactions remains both relatively unexplored and interesting to us—namely, the interaction of *carbocationic* centers with the π-faces of aromatic rings in proximity (Figure 1). From a biochemical perspective, a few

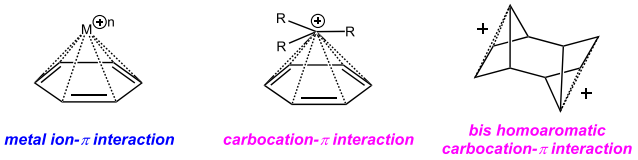

Figure 1. Generalized aryl cation−π interactions and an example of carbocation−π interacting system.

intriguing X-ray structural studies of enzymatic systems suggest that key aromatic amino acid residues play a role in stabilizing carbocation intermediates.[4,12−15] Being coordinatively unsaturated, carbocations are expected to interact somewhat differently with π-systems than ammonium cations, for example.[16−19] On the other hand, experimental examples of chemical systems that explore the nature of carbocation−π interactions in aromatic systems are fairly rare.[20]

In this note, we present an unusual carbocation resulting from protonation at the carbonyl oxygen of a recently reported *para*-quinone methide (p-QM **1**, Figure 2).[21] NMR, UV−vis, and

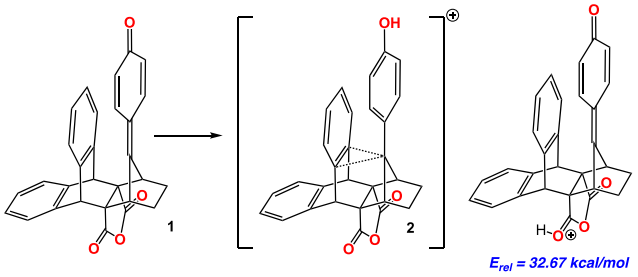

Figure 2. Protonation of **1**, and the relative stability of the anhydrido-protonated form at ωB97XD/6-311+G**.

crystallographic analyses show that the protonated form is stabilized not only by the expected partial aromatization of the p-QM moiety, but also by a mild through-space, π−cation interaction with the proximate aromatic ring. Single crystal X-ray analysis revealed an interesting structure consisting of a hydrogen-bound complex involving two molecules of the precursor and one shared proton.

Previous studies reveal that under acidic conditions, relatively stable p-QM's undergo solvolysis through 1,6-addition. For example, 2,6,7,7-tetralkyl-substituted p-QM's undergo spontaneous alcoholysis when treated with acids in MeOH.[22] The high

Received: April 3, 2019
Published: May 22, 2019

DOI: 10.1021/acs.joc.9b00923
J. Org. Chem. 2019, 84, 8284−8288

stability of p-QM **1** suggested to us that it instead would prove refractory to discrete methanolysis under similar conditions. Although true enough, it provided the first experimental hint of the facile protonation of **1**. A lemon-yellow solution of p-QM **1** in methanol instantly turned dark amber upon the addition of a drop of concentrated sulfuric acid, indicative of possible carbocation formation; even when stirred at room temperature for 24 h, **1** was recovered quantitatively after workup. We hypothesized that the color change corresponded to the protonation of the QM-carbonyl oxygen rather than protonation of an anhydride oxygen. Our hypothesis was backed by DFT calculations at ωB97XD/6-311+G** that predicts the carbonyl oxygen to be the most basic site in **1** by a large measure (Figure 2).

The resultant cation **2** is also calculated to be some 35.8 and 16.4 kcal/mol more stable than the reactants for protonated acetone and benzophenone. More importantly, calculations predict a direct correlation between the electronic nature of the neighboring aromatic ring and the basicity of the QM moiety, i.e., the more electron rich the aromatic ring, the more basic the QM carbonyl group, suggesting the possibility for a fruitful carbocation–π interaction. The isodesmic relation[23] (Scheme 1) was calculated to be *exothermic* by 3.4 kcal/mol when the

Scheme 1. Isodesmic Relation Comparing p-QM 1 with Substituted Forms

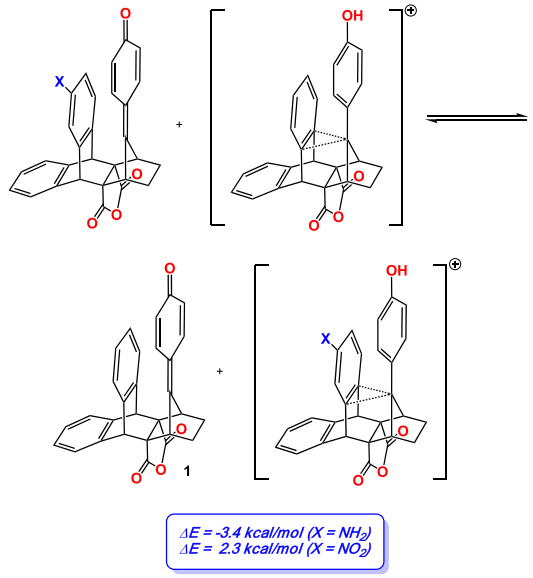

neighboring aromatic ring contains an amino group in the top position (X = NH_2) and *endothermic* by 2.3 kcal/mol when it possesses a nitro group at the same position (X = NO_2). Thus, a combination of partial aromatization and delocalization of positive charge onto the proximate aromatic ring seems to account for the predicted basicity of **1**. Interestingly, DFT calculations (ωB97XD/6-311+G**) also predict the carbonyl oxygen to be more basic than the aniline nitrogen of the top-amine version of p-QM **1** by 8.4 kcal/mol in vacuum and by 2.5 kcal/mol in acetonitrile (IEFPCM solvent model) (Figure 3).

Experimentally, a variety of protic acids and solvents were sampled in order to ascertain an optimal system for spectroscopic characterization. Initial trial experiments revealed acetonitrile to be the most flexible solvent for this purpose. Thereupon, we screened acetic acid, trifluoroacetic acid and triflic acid for their protonating ability. ^{1}H NMR analysis of p-QM **1** treated with all

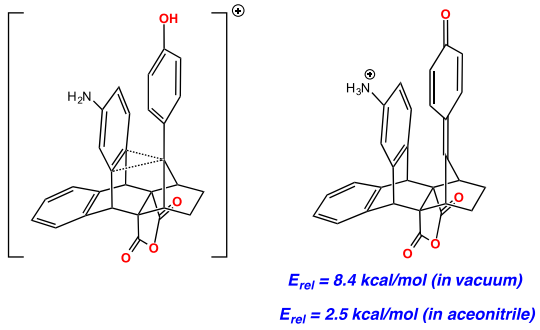

Figure 3. Protonation of the carbonyl oxygen vs aniline nitrogen.

three protic acids suggests a fast exchange process in MeCN at the carbonyl oxygen of **1** at room temperature. The changes in the proton chemical shifts of the QM moiety of **1** are moderate in CH_3COOH, intermediate in CF_3COOH, whereas limiting values are reached in TfOH (Figure 4).

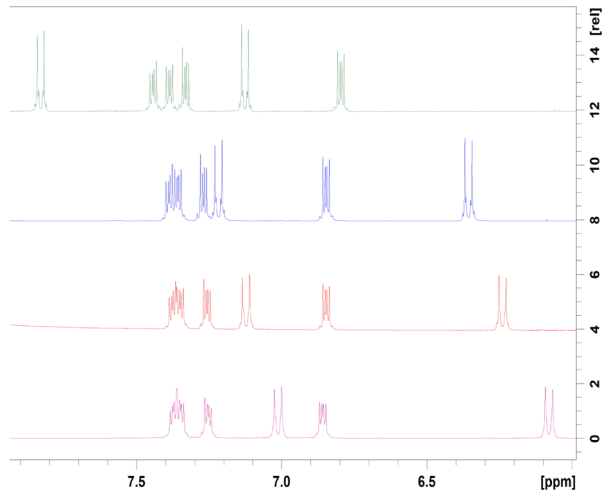

Figure 4. Behavior of aromatic and QM protons when p-QM **1** is treated with different acids in CD_3CN. Doublets indicate protons on the QM fragment and multiplets represent protons on the aromatic rings. Bottom to top: p-QM **1**, p-QM **1** with acetic acid, p-QM **1** with trifluoroacetic acid, p-QM **1** with triflic acid.

When treated with only 2 equiv of triflic acid in CD_3CN at room temperature, the corresponding carbocation **2** forms cleanly (Scheme 2). The ^{1}H NMR (in CD_3CN) clearly demonstrates the protonation of **1** at the carbonyl oxygen. The protons on the QM moiety are perturbed to a greater extent (6.07 to 7.14 ppm, and 7.01 to 7.83 ppm) than the aromatic protons (6.79 to 6.86 ppm, 7.25 to 7.32 ppm, 7.35 to 7.38 ppm, and 7.37

Scheme 2. Protonation of p-QM 1

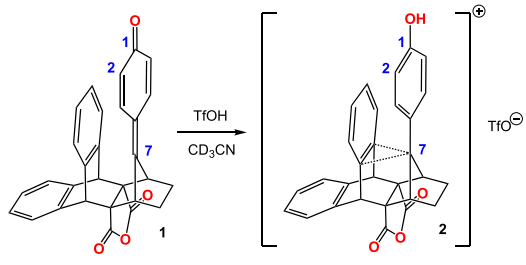

DOI: 10.1021/acs.joc.9b00923
J. Org. Chem. 2019, 84, 8284–8288

to 7.44 ppm) (Figure 4). Similar trends are observed for both benzylic and aliphatic bridge protons (4.84 to 5.0 ppm, and 3.59 to 4.01 ppm, respectively), the latter being affected to a greater extent indicating their proximity to the cationic site in the molecule (Figure 5).

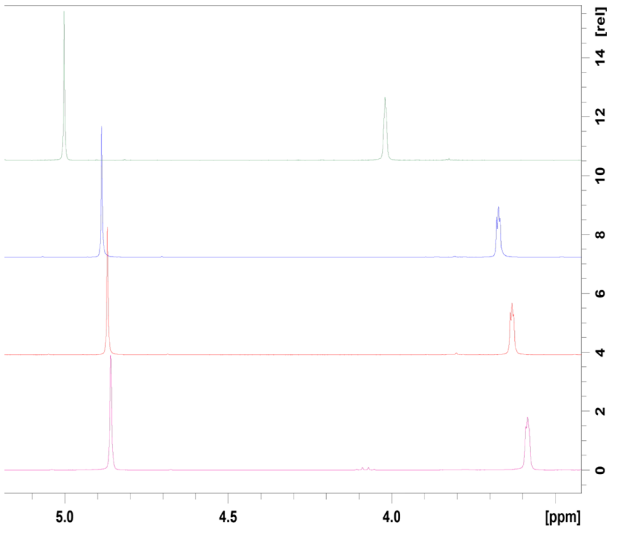

Figure 5. Behavior of the bridge protons when p-QM **1** is treated with different acids in CD_3CN. Protons in the region 3.5−4 ppm represent the bridge protons near the QM fragment while those in the region 4.8−5.1 ppm represent the benzylic bridge protons. Bottom to top: p-QM **1**, p-QM **1** with acetic acid, p-QM **1** with trifluoroacetic acid, p-QM **1** with triflic acid.

Nevertheless, this apparent fast exchange in the ^1H NMR spectrum suggested that ^{13}C NMR would be more illustrative, as chemical shifts could be more accurately calculated for comparison. The ^{13}C NMR resonance of the QM carbonyl group shifts upfield to 149.4 ppm, which is in agreement with the calculated ^{13}C NMR value for this carbon (calc. 149 ppm at B3LYP/6-311++G**; see Supporting Information). Conversely, the trisubstituted alkenyl, now a trisubstituted alkyl, carbon moves strongly downfield (204 ppm), consistent with the calculated ^{13}C NMR resonance value for this carbon (calc. 202 ppm at B3LYP/6-311++G**). The ^{13}C chemical shifts of the nearby aromatic ring are affected as well, albeit to a lesser extent. ^{13}C NMR spectra of **1** in the presence of HOAc and TFA are slightly changed, but only in the presence of TfOH are substantial, limiting shifts comparable to calculation noted. Taken together, the chemical shift data point to protonation by TfOH to form **2**, wherein partial aromatization of the QM moiety, and modest delocalization of charge on the proximate aromatic ring through a π-interaction focused at carbon 7 occur.

p-QM **1** exhibits two absorption maxima at 281 and 337 nm in the UV−vis spectrum (MeCN); in contrast, cation **2** shows three absorption peaks at 283, 339, and 417 nm (Figure 6). The new absorption in the visible region can be accounted for by preferential lowering of the primarily QM-centered LUMO upon protonation at the QM carbonyl group.

Another illuminating piece of data was provided by X-ray crystallographic analysis. Interestingly, the unit cell contains cation **2** stabilized by hydrogen bonding to other QM carbonyl oxygen atoms (Scheme 2 and Figure 9). Changes in bond lengths (e.g., the C_1-C_2 bond attached to the p-QM carbonyl shrinks from 1.457 Å in the p-QM **1** to 1.431 and 1.433 Å in the QM

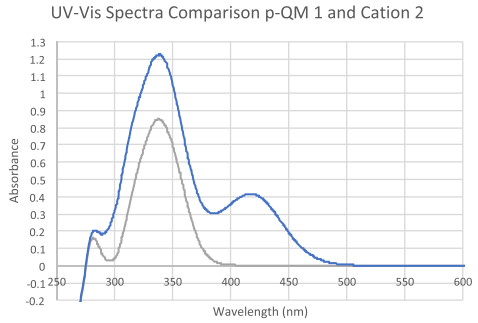

Figure 6. UV−vis spectra of p-QM **1** (gray) and cation **2** (blue) in MeCN.

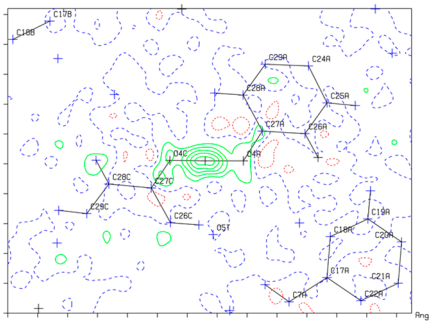

Figure 7. Contoured Fourier map of the proton shared by the two p-QM molecules (O4A and O4C represent the carbonyl oxygen atoms of the QM moieties).

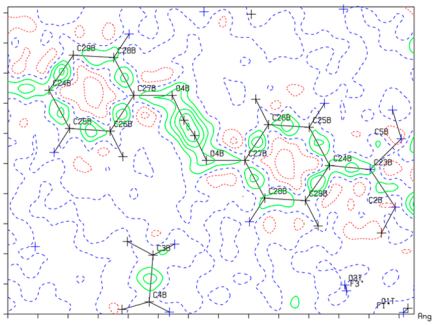

Figure 8. Contoured Fourier map of the independent hydrogen bound proton (O4B represents the carbonyl oxygen of the QM attached to the proton, whereas O4B* denotes the oxygen atom on QM generated by the Mercury program).

molecules sharing the proton and 1.431 Å in the independent half protonated QM upon protonation) and interatomic distances are also consistent with partial aromatization of the QM moiety and some through-space delocalization of charge (approach of C_7 to the adjacent aromatic ring carbons changes from 2.894, 2.939 Å in the parent p-QM **1** to 2.842, 2.860 Å and 2.866, 2.860 Å in the QMs sharing the proton and 2.857, 2.864 Å in the independent half protonated QM molecule).

The crystallographic analysis of a single unit also shows the existence of one and a half triflate ions that carry an overall charge of −1.5. The data were consistent with the existence of two electron density peaks, carrying an overall charge of +1.5 representing the two protons found near the carbonyl oxygens on the QM fragments. One of those peaks is found approximately equidistant from O4A and O4C, which suggests that one H atom is shared with both O atoms (Figure 7). However, the other proton peak is attached to O4B, which is donor to O4B* (O4B*

DOI: 10.1021/acs.joc.9b00923
J. Org. Chem. 2019, 84, 8284−8288

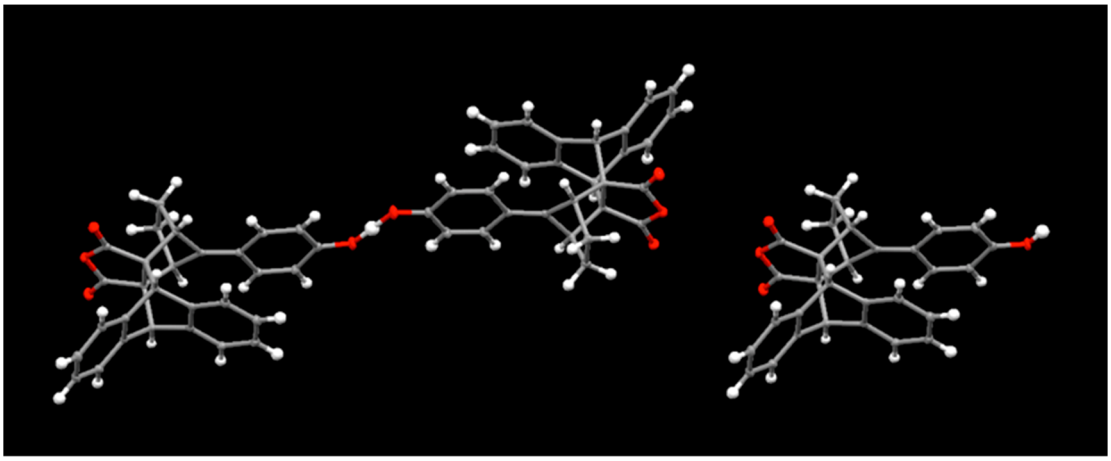

Figure 9. Crystal structure of the protonated-hydrogen bonded forms of p-QM **1**. The asymmetric crystal unit contains three target molecules and one and a half triflate counterions (TfO^- counterions have been removed for clarity).

= O atom related to O4B by one inversion center), and its occupancy factor must be 0.5 as there would be an impossibly short O4B−H4B···H4B*−O4B* (the starred atoms are generated by inversion symmetry) contact otherwise. Contoured difference Fourier maps show unequivocally the existence of those two peaks (Figure 8).

Finally, we turned back to DFT calculations in order to compare the X-ray structure with an optimized geometry for a carbocation−π interaction in a system resembling cation **2** but lacking structural constraints. DFT calculations (at ωB97XD/6-311+G**) predict that in model system A (Figure 10), the carbocation−π interaction manifests itself similarly, although with stricter coplanarity of the aromatic and p-QM rings and loss of C_s symmetry (see Supporting Information for details).

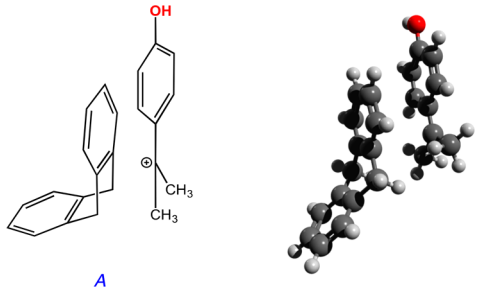

Figure 10. Model system **A** used for comparing the optimized geometry of carbocation−π interactions with cation **2** and its optimized geometry at ωB97XD/6-311+G**.

CONCLUSION

We have reported the spectroscopic and crystallographic analysis of a cation generated by the facile protonation of aliphatic p-QM **1**. Both calculations and experimental data suggest that it is stabilized by partial aromatization of the QM fragment as well as a modest through-space carbocation−π interaction with the neighboring aromatic ring. A single crystallographic unit contains three p-QM molecules sharing two protons with an overall charge of +1.5, along with one and a half triflate counterions. Finally, this protonated p-QM provides a rare experimental example of a simple, crystallizable chemical system that allows the direct study of a carbocation−π interaction.

EXPERIMENTAL SECTION

Synthesis of the p-QM (Compound 1). Compound **1** (p-QM) was synthesized following the previously reported method.[21]

Generation of the Protonated p-QM. Compound **1** (15 mg, 0.035 mmol) was dissolved in 1 mL of CD_3CN in an NMR tube, and 2 equiv of trifluoromethanesulfonic acid (TfOH) were added to the tube. The light-yellow solution immediately turned dark amber. The sample was transferred to a vial and set aside for crystallization, which yielded yellow crystals over a matter of days: ^{1}H NMR (CD_3CN) δ 12.5 (s, broad) 7.83 (d, 2H, 9.3 Hz), 7.43−7.44 (q, 2H), 7.38−7.39 (q, 2H), 7.32−7.33 (q, 2H), 7.135 (d, 2H, 9.3 Hz), 4.99−5.0 (s, 2H), 4.01 (m, 2H), 1.81 (m, 4H); ^{13}C{^{1}H} NMR δ 204.7, 181.0, 169.7, 149.5, 139.3, 137.2, 130.1, 128.4, 127.3, 125.6, 123.0, 121.0, 120.5, 66.3, 47.8, 47.4, 22.3.

ASSOCIATED CONTENT

Supporting Information

The Supporting Information is available free of charge on the ACS Publications website at DOI: 10.1021/acs.joc.9b00923.

Crystal structure data, NMR spectra, and computational information (PDF)

Crystal structure for compound **1** (CCDC 1897938) (CIF)

Crystal structure for cation **2** (CCDC 1907578) (CIF)

AUTHOR INFORMATION

Corresponding Author

*E-mail: lectka@jhu.edu.

ORCID

Muhammad Kazim: 0000-0003-2020-8952

Notes

The authors declare no competing financial interest.

ACKNOWLEDGMENTS

T.L. thanks the National Science Foundation (NSF) (Grant CHE 90079165) for financial support. The authors thank Professor J. D. Tovar for the use of his UV−vis spectrometer and Professor Lan Cheng for helpful discussions with computations.

REFERENCES

(1) Mahadevi, A. S.; Sastry, G. N. Cation−π Interaction: Its Role and Relevance in Chemistry, Biology, and Material Science. *Chem. Rev.* **2013**, *113*, 2100−2138.

DOI: 10.1021/acs.joc.9b00923
J. Org. Chem. 2019, 84, 8284−8288

(2) Hong, B. H.; Bae, S. C.; Lee, C. W.; Jeong, S.; Kim, K. S. Ultrathin Single-Crystalline Silver Nanowire Arrays Formed in an Ambient Solution Phase. *Science* **2001**, *294*, 348−351.
(3) Dougherty, D. A. The Cation-π Interaction. *Acc. Chem. Res.* **2013**, *46*, 885−893.
(4) Faraldos, J. A.; Antonczak, A. K.; Gonzalez, V.; Fullerton, R.; Tippmann, E. M.; Allemann, R. K. Probing eudesmane cation-π interactions in catalysis by aristolochene synthase with non-canonical amino acids. *J. Am. Chem. Soc.* **2011**, *133*, 13906−13909.
(5) Dougherty, D. A. Cation-π Interactions in Chemistry and Biology: A New View of Benzene, Phe, Tyr, and Trp. *Science* **1996**, *271*, 163−168.
(6) Torrice, M. M.; Bower, K. S.; Lester, H. A.; Dougherty, D. A. Probing the role of the cation-pi interaction in the binding sites of GPCRs using unnatural amino acids. *Proc. Natl. Acad. Sci. U. S. A.* **2009**, *106*, 11919−11924.
(7) Sunner, J.; Nishizawa, K.; Kebarle, P. Ion-Solvent Molecule Interactions in the Gas Phase. The Potassium Ion and Benzene. *J. Phys. Chem.* **1981**, *85*, 1814−1820.
(8) Kim, D.; Hu, S.; Tarakeshwar, P.; Kim, K. S. Cation−π Interactions: A Theoretical Investigation of the Interaction of Metallic and Organic Cations with Alkenes, Arenes, and Heteroarenes. *J. Phys. Chem. A* **2003**, *107*, 1228−1238.
(9) Shepodd, T. J.; Petti, M. A.; Dougherty, D. A. Tight Oriented Binding of an Aliphatic Guest by a New Class of Water-Soluble Molecules with Hydrophobic Binding Sites. *J. Am. Chem. Soc.* **1986**, *108*, 6085−6087.
(10) Petti, M. A.; Shepodd, T. J.; Barrans, R. E.; Dougherty, D. A. Hydrophobic" Binding of Water-Soluble Guests by High-Symmetry, Chiral Hosts. An Electron-Rich Receptor Site with a General Affinity for Quaternary Ammonium Compounds and Electron-Deficient π-Systems. *J. Am. Chem. Soc.* **1988**, *110*, 6825−6840.
(11) Kearney, P. C.; Mizoue, L. S.; Kumpf, R. A.; Forman, J. E.; McCurdy, A.; Dougherty, D. A. Molecular recognition in aqueous media. New binding studies provide further insights into the cation-pi interaction and related phenomena. *J. Am. Chem. Soc.* **1993**, *115*, 9907−9919.
(12) Christianson, D. W. Structural biology and chemistry of the terpenoid cyclases. *Chem. Rev.* **2006**, *106*, 3412−3442.
(13) Chang, C. H.; Wen, H. Y.; Shie, W. S.; Lu, C. T.; Li, M. E.; Liu, Y. T.; Li, W. H.; Wu, T. K. Protein engineering of oxidosqualene-lanosterol cyclase into triterpene monocyclase. *Org. Biomol. Chem.* **2013**, *11*, 4214−4219.
(14) Ito, R.; Hashimoto, I.; Masukawa, Y.; Hoshino, T. Effect of cation-pi interactions and steric bulk on the catalytic action of oxidosqualene cyclase: a case study of Phe728 of beta-amyrin synthase from Euphorbia tirucalli L. *Chem. - Eur. J.* **2013**, *19*, 17150−17158.
(15) Ma, J. C.; Dougherty, D. A. The Cation−π Interaction. *Chem. Rev.* **1997**, *97*, 1303−1324.
(16) Miklis, P. C.; Ditchfield, R.; Spencer, T. A. Carbocation-π Interaction: Computational Study of Complexation of Methyl Cation with Benzene and Comparisons with Related Systems. *J. Am. Chem. Soc.* **1998**, *120*, 10482−10489.
(17) Oliveira, F. G.; Esteves, P. M. Interaction of Allylic Carbocations with Benzene: a Theoretical Model of Carbocationic Intermediates in Terpene Biosynthesis. *J. Braz. Chem. Soc.* **2011**, *22*, 1979−1986.
(18) Ditchfield, R.; Spencer, T. A. Carbocation-π interaction: the 1,1-dimethylallyl cation and benzene. *Tetrahedron Lett.* **2011**, *52*, 3674−3677.
(19) Ditchfield, R.; Spencer, T. A. Carbocation−π interaction: evaluation of the stabilization by phenylalanine of a biochemical carbocation intermediate. *Org. Biomol. Chem.* **2016**, *14*, 9543−9548.
(20) Prakash, G. K. S.; Farnia, M.; Keyanian, S.; Olah, G. A.; Kuhn, H. J.; Schaffner, K. The anti-tricyclo[4.2.1.12,5]deca-3,7-diene-9,10-diyl dication: a sandwiched bishomoaromatic system. *J. Am. Chem. Soc.* **1987**, *109*, 911−912.
(21) Kazim, M.; Siegler, M. A.; Lectka, T. A Case of Serendipity: Synthesis, Characterization, and Unique Chemistry of a Stable, Ring-Unsubstituted Aliphatic p-Quinone Methide. *Org. Lett.* **2019**, *21*, 2326−2329.
(22) Cook, C. D.; Norcross, B. E. Oxidation of Hindered Phenols. V. The 2,6-Di-t-butyl-4-isopropyl and −4-sec-Butylphenoxy Radicals. *J. Am. Chem. Soc.* **1956**, *78*, 3797−3799.
(23) Hehre, W. J.; Ditchfield, R.; Radom, L.; Pople, J. A. Molecular orbital theory of the electronic structure of organic compounds. V. Molecular theory of bond separation. *J. Am. Chem. Soc.* **1970**, *92*, 4796−4801.

DOI: 10.1021/acs.joc.9b00923
J. Org. Chem. 2019, 84, 8284−8288